Prabha Materials Science Letters
Vol. 5, No. 1, 185-206, 2026
https://doi.org/10.33889/PMSL.2026.5.1.010

Spectroscopic Analysis of 2-Phthalimidoethanesulfonyl Chloride by Density Functional Theory

B. S. Yadav
Department of Physics,
Molecular Spectroscopy and Biophysics Laboratory,
Deva Nagri College, Chaudhary Charan Singh University, Meerut, 250002, Uttar Pradesh, India.
E-mail: bijendrasyadav@gmail.com

Chanchal Chauhan
Department of Physics,
Molecular Spectroscopy and Biophysics Laboratory,
Deva Nagri College, Chaudhary Charan Singh University, Meerut, 250002, Uttar Pradesh, India.
E-mail: chanchallch2@gmail.com

Sarvendra Kumar
Department of Physics,
SRM Institute of Science and Technology,
Delhi NCR Campus, Modinagar, 201204, Uttar Pradesh, India.
Corresponding author: sarvendraricky@gmail.com, sarvendk1@srmist.edu.in

Jayant Teotia
Department of Physics,
Molecular Spectroscopy and Biophysics Laboratory,
Deva Nagri College, Chaudhary Charan Singh University, Meerut, 250002, Uttar Pradesh, India.
E-mail: jayant.phy@gmail.com

Shalini Malik
Department of Physics,
Dr Akhilesh Das Gupta Institute of Professional Studies, Dwarka, New Delhi, India.
E-mail: drshaliniphy@gmail.com

Megha Gupta Chaudhary
Department of Physics,
Gurukul Kangri University, Haridwar, Uttarakhand, India.
E-mail: tomeghag@gmail.com

Dev Kumar
Department of Chemistry,
National Changhua University of Education, Changhua 500, Taiwan.
E-mail: devkumar100394@gmail.com

(Received on November 13, 2025; Revised on February 25, 2026; Accepted on March 2, 2026)

Abstract
Density Functional Theory (DFT) computations are used to analyse 2-phthalimidoethanesulfonyl chloride (2-PESC). DFT computations are performed using the B3LYP method with 6-311++G (d,p) and cc-pVDZ core levels. The structural properties of the examined molecule, such as interatomic distances and the angle between bonds, are theoretically calculated using DFT. Heat capacity, entropy, and enthalpy—the three thermodynamic parametersare parameters are for a temperature range from 100

to 1000 Kelvin. DFT is used to compute the molecule's first and second-order hyperpolarizability (nonlinear optical NLO characteristics) at both basis sets. With the help of the VEDA program, assignments are computed. The Swiss ADME tool is used to analyze the molecule (2-PESC) for drug likeness. FT-IR and FT-Raman are used to characterize the molecule's vibrational spectra in the domains of 4000-650 cm^{-1} and 4000-100 cm^{-1}, respectively. The hybridization and covalent effects are examined using the Natural Bond Orbital (NBO) technique. Lastly, Mulliken atomic charges of the atoms are also computed.

Keywords- 2-Phthalimidoethanesulfonyl chloride, Thermodynamic functions, Density functional theory.

1. Introduction

Phthalimide (isoindole-1, 3-diones) is an organic and aromatic substance. Nitrogen is one of its heteroatoms. It is a member of the nitrogen-containing group. Phthalic anhydride is used to make it. It has an acidic character, and resonance stabilises its conjugate base. The structure gains additional stability from resonance (Kushwaha and Kaushik, 2016). NBO, thermodynamic parameters and applications of phthalimide derivatives have been studied (Balachandran et al., 2012). Phthalimide derivatives are used in the manufacture of antimicrobial products, antiandrogens, and other medications used to treat tumor necrosis factor (Krishnakumar et al., 2005; Santos et al., 2009; Akgün et al., 2012; Evecen et al., 2016; Doraghi et al., 2024; Udayappan et al., 2024). Some phthalimide derivatives are used to reduce bacterial contamination and are used as herbicides. On the industrial side, they function as flame-retardants, heat-resistant polymers, antidepressants, bleaching detergents, and anion exchange resins, among others (Krishnakumar et al., 2005). Phthalimides have several uses in medicine, but they also have promising prospects in the dye, polymer, and agrochemical sectors. It was recently reported that phthalimide was used in the production of rubber, dyestuff, and insecticides. Phthalimides have important roles in medicinal chemistry as anti-convulsive, nonsteroidal drugs, painkillers, anti-hyperlipidemic drugs, and immunomodulatory agents (Sharma et al., 2010) in addition to their well-known uses in pharmaceuticals (Karthick et al., 2011).

According to recent reports, compounds of phthalimide have anticholinesterase properties. The literature claims that compounds based on phthalimide have demonstrated their ability to interact with the acetylcholinesterase enzyme's CAS (catalytic active site) and PAS (peripheral anionic site) (Aygün et al., 2024).

Due to the many applications of Phthalimide derivatives, the current work focuses on 2-phthalimidoethanesulfonyl chloride (2-PESC). To analyse structural components, thermodynamic quantities, Natural Bond Orbital (NBO) evaluation, Non-linear optical (NLO) characteristics, DFT simulations are utilised for the study of the 2-phthalimidoethanesulfonyl chloride (2-PESC) molecule.

The substance 2-phthalimidoethanesulfonyl chloride (2-PESC) is an organic compound formulated as $C_{10}H_8Cl\ NO_4S$. It has an ethyl group that has been substituted with a phthalimide, which means that it is a sulfonyl chloride derivative. This substance serves as a crucial bridge in the production of several colours, agrochemicals, and medicines. The chemical is susceptible to moisture. It is known to be caustic and reacts with water. The melting point of the molecule is 162°C. It serves as an intermediate in chemical synthesis, particularly for the production of 2-substituted-phthalimide derivatives, and is typically categorised as a pharmacological building block. The substance 2-phthalimidoethanesulfonyl chloride (2-PESC) was used as such without further purification after being bought from Tokyo Chemical Ltd. with a reported purity of 99 percent. (2-PESC) is a phthalimide based derivative with molecular formula $C_{10}H_8ClNO_4S$.

2. Computational Details

As technology has advanced, computational techniques have made it possible for the scientific community to use computer simulations and algorithms to efficiently synthesize new chemicals and understand chemical difficulties. The Gaussian 09 software package is used for Density functional theory (DFT) computational calculations. Different basis sets can be used for DFT computations. This study uses the core levels B3LYP/6-311++G(d,p) and B3LYP/cc-pVDZ, which are capable of producing better results as compared to other basis sets. Here (LYP) Lee-Yang-Parr correlation functional and (B3) Becke's three-parameter exchange functional, B3LYP have been utilized (Lee et al., 1988).

The Gauss view software is used to visualize the molecule's structure and aids in the analysis of the parameters determined by DFT. Thermodynamic parameters (heat capacity, entropy, and enthalpy) are computed for a temperature range of 100K to 1000K using the B3LYP/6-311++G(d,p) core level. The NLO (nonlinear optical) properties are computed at B3LYP/6-311++G(d,p) and B3LYP/cc-pVDZ core levels. The interatomic distance and bond angles of the optimized molecule (2-PESC) are computed at the B3LYP/6-311++G(d,p) and B3LYP/cc-pVDZ core levels. The SwissADME tool (Daina et al., 2017) is utilized to determine the biological effect of the compound (2-PESC).

3. Drug Likeliness

Drug-likeliness supports drug discovery by assisting in the computation of physiochemical descriptors and the analysis of pharmacokinetic features for use in the pharmaceutical industry. Lipinski's rule of five must be followed by the compound for there to be a high likelihood of drug similarity (Lipinski, 2004). Based on **Table 1**, the molecule (2-PESC) exhibits a strong biological availability score of 0.55 without violating the Lipinski rule. To calculate all of these physiochemical characteristics, the Swiss ADME tool (Daina et al., 2017) was utilized. Therefore, the molecule (2-PESC) is suitable for use in the medical field.

Table 1. Drug likeliness of the (2-PESC) molecule.

Descriptor value	Value
HBD - Hydrogen Bond Donor	0
HBA - Hydrogen Bond Acceptor	4
TPSA - Topological polar surface area [$Å^2$]	79.90
Number of heavy atoms	17
Number of hydrogen atoms	8
Number of rotatable bonds	3
Molecular weight	273.69
Bioavailability score	0.55

This molecule primarily functions as a versatile linker. It significantly influences the permeability and bioavailability of small molecule drugs. Its main function in drug design is to serve as a construction block for sulfonamide-linked derivatives, which are frequently employed to enhance pharmacological effects. In order to create more complicated and stable compounds, it is mostly used as a synthetic precursor.

In the molecule 2-PESC, the phthalimide ring increases the lipophilicity of the molecule and increased lipophilicity can enhance the permeability. Phthalimide acts as a notable lipophilic "mask" during the initial phases of drug synthesis or as a prodrug moiety. The sulfonyl group in this molecule improves metabolic stability. This building block is used in derivatives that are often studied for their anti-inflammatory, antibacterial, and anticancer properties, demonstrating their versatility in enhancing bioavailability in a range of therapeutic domains.

4. Structural Parameters

Figure 1 shows the structure and atom numbering of the 2-PESC molecule. By using DFT calculations, the molecule's optimal geometry is determined, and **Table 2** displays the optimised bond angles and bond lengths with the B3LYP/6-311++G(d,p) and B3LYP/cc-pVDZ sets.

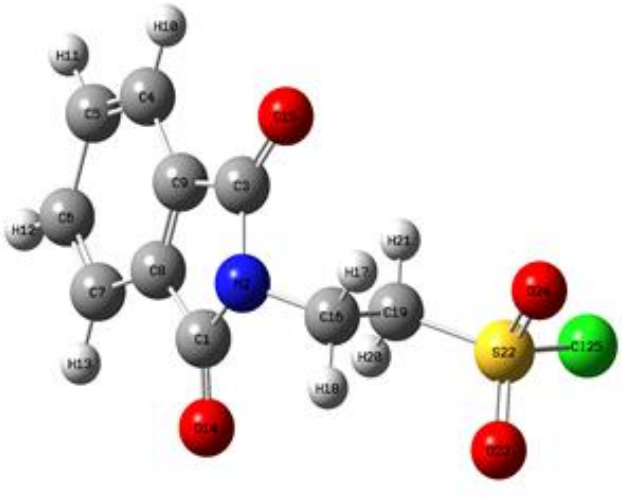

Figure 1. The optimized structure of the molecule (2-PESC) with atom numbering.

The minimum atomic separation is 1.080 Å for the C7-H13 atom at B3LYP/ 6-311++G (d,p) set and the maximum atomic separation is 2.397 Å for the S22-Cl25 atom at B3LYP/6-311++G(d,p) set.

For C-C pair, the lowest atomic separation is 1.386 Å for the C4-C9 atom at B3LYP/6-311++G(d,p) set. The highest atomic separation is 1.538 Å for the C16-C19 atom at B3LYP/ cc-pVDZ set. At B3LYP/6-311++G (d,p) set, the atomic separation between C1-C8 & C3-C9 atoms is 1.484 Å, and at the B3LYP/cc-pVDZ set, it is 1.4931 Å.

For the C-H pair, the bond length between C4-H10 atom and C7-H13 atom is 1.081 Å & 1.091 Å at B3LYP/ 6-311++G(d,p) and B3LYP/ cc-pVDZ, respectively. For C6-H12, the bond length is 1.081Å and 1.092Å at B3LYP/6-311++G(d,p) and B3LYP/cc-pVDZ sets, respectively. The atomic separation for C16-H17 and C16-H18 atoms is 1.088 & 1.098 at B3LYP/ 6-311++G(d,p) and B3LYP/cc-pVDZ sets, respectively. Similarly, for the C19-H20 & C19-H21 atom, the bond length is 1.085 Å and 1.098 Å at B3LYP/6-311++G(d,p) and B3LYP/cc-pVDZ sets respectively. The C1-O14 and C3-O15 atoms in both sets have interatomic distances ranging from 1.235 Å to 1.212 Å for C-O interactions. The interatomic distance between N2-C3 for the C-N interaction is calculated as 1.418 Å and 1.410 Å with B3LYP/6-311++G(d,p) and B3LYP/cc-pVDZ sets, respectively. Similarly, the interatomic distance between N2-C16 atom is 1.455 Å & 1.449 Å at B3LYP/6-311++G(d,p) and B3LYP/ cc-pVDZ sets respectively. For C-S interaction, the C19-S22 interatomic distance is 1.934 Å and 1.825 Å at B3LYP/6-311++G(d,p) and B3LYP/cc-pVDZ sets, respectively. The interatomic distance between the S22-O23 and S22-O24 atoms for the S-O interaction are same, measuring 1.618 Å and 1.473 Å at the B3LYP/ 6-311++G (d,p) and B3LYP/ cc-pVDZ sets, respectively. For S-Cl interaction, the bond length is 2.397 Å at B3LYP/ 6-311++G(d,p) set and 2.158 Å at B3LYP/ cc-pVDZ set.

According to **Table 2** of the bond angle of compound (2-PESC), the lowest bond angles for C19-S22-Cl25 at B3LYP/6-311++G(d,p) and B3LYP/cc-pVDZ sets are 97.30˚ and 98.83˚, respectively, while the largest bond angles for C8-C1-O4 and C9-C3-O15 at B3LYP/6-311++G (d,p) set are 130.16˚. The bond angle between C8-C1-O4 and C9-C3-O15 is 130.16˚ at B3LYP/ 6-311++G(d,p) set and 129.84˚ at B3LYP/ cc-pVDZ set. The C-C-C bond angle is of the order of 108˚ for C3-C9-C8 and C1-C8-C9, and is of the order of 130˚ for C1-C8-C7 and C3-C9-C4 at both basis sets. The bond angle between C19-S22-O23 & C19-S22-O24 is 109.48˚ & 109.57˚ at B3LYP/6-311++G(d,p) and B3LYP/cc-pVDZ set, respectively. O23-S22-Cl25 and O24-S22-Cl25 have bond angles of 108.33˚ and 107.24˚ at B3LYP/6-311++G(d,p) and B3LYP/cc-pVDZ sets, respectively. For H20-C19-S22 and H21-C19-S22, the bond angle is 102.75˚ at B3LYP/6-311++G(d,p) and 105.64˚ at B3LYP/cc-pVDZ set, respectively. The N-C-H has a bond angle of 108.53˚ and 108.24˚ at B3LYP/6-311++G (d,p) and B3LYP/cc-pVDZ sets, respectively. In the B3LYP/6-311++G (d,p) set, the bond angle between C-C-H varies from 119.44˚ for C6-C5-H11 to 121.50˚ for C5-C4-H10. At B3LYP/ 6-311++G(d,p) and B3LYP/cc-pVDZ sets, the bond angle for N-C-O is 124.34˚ and 124.80˚, respectively. Similarly, in B3LYP/ 6-311++G (d,p) and B3LYP/ cc-pVDZ sets, the bond angle for N-C-C is 105.50˚ and 105.36˚, respectively. The bond angle for C1-N2-C3 at B3LYP/6-311++G(d,p) and B3LYP/cc-pVDZ sets, respectively, is between 111.86˚ and 112.40˚. Both C1-N2-C16 and C3-N2-C16 have the same bond angle, which is 123.80˚ at B3LYP/cc-pVDZ set and 124.05˚ at B3LYP/6-311++G(d,p) set.

It is clear from the above calculation that the bond angles determined at B3LYP/6-311++G(d,p) set are slightly greater than those determined at the B3LYP/ cc-pVDZ set.

Table 2. The optimised bond length and bond angle for the molecule (2-PESC) calculated at B3LYP/cc-pVDZ and B3LYP/6-311++G (d,p) basis sets.

Bond Length (Å)	B3LYP/ 6-311++G(d, p)	B3LYP/ cc-pVDZ	Bond Angle (°)	B3LYP/ 6-311++ G(d,p)	B3LYP/ cc-pVDZ
C1-N2	1.418	1.410	N2-C1-C8	105.50	105.36
C1-C8	1.484	1.493	N2-C1-O14	124.34	124.80
C1-O14	1.235	1.212	C8-C1-O14	130.16	129.84
N2-C3	1.418	1.410	C1-N2-C3	111.86	112.40
N2-C16	1.455	1.449	C1-N2-C16	124.05	123.80
C3-C9	1.484	1.493	C3-N2-C16	124.05	123.80
C3-O15	1.235	1.212	N2-C3-C9	105.50	105.36
C4-C5	1.404	1.403	N2-C3-O15	124.34	124.80
C4-C9	1.386	1.390	C9-C3-O15	130.16	129.84
C4-H10	1.081	1.091	C5-C4-C9	117.57	117.38
C5-C6	1.401	1.403	C5-C4-H10	121.50	121.77
C5-H11	1.081	1.092	C9-C4-H10	120.93	120.85
C6-C7	1.404	1.403	C4-C5-C6	121.04	121.10
C6-H12	1.081	1.092	C4-C5-H11	119.52	119.58
C7-C8	1.386	1.387	C6-C5-H11	119.44	119.32
C7-H13	1.081	1.091	C5-C6-C7	121.04	121.10
C8-C9	1.404	1.399	C5-C6-H12	119.44	119.32
C16-H17	1.088	1.098	C7-C6-H12	119.52	119.58
C16-H18	1.088	1.098	C6-C7-C8	117.57	117.38
C16-C19	1.531	1.538	C6-C7-C13	121.50	121.77
C19-H20	1.085	1.098	C8-C7-C13	120.93	120.85
C19-H21	1.085	1.098	C1-C8-C7	130.04	130.04
C19-S22	1.934	1.825	C1-C8-C9	108.57	108.44
S22-O23	1.618	1.473	C7-C8-C9	121.39	121.52
S22-O24	1.618	1.473	C3-C9-C4	130.04	130.04
S22-Cl25	2.397	2.158	C3-C9-C8	108.57	108.44
			C4-C9-C8	121.39	121.52
			N2-C16-H17	108.53	108.24
			N2-C16-H18	108.53	108.24

Table 2 continued…

			N2-C16-C19	108.73	110.51
			H17-C16-H18	110.00	110.00
			H17-C16-C19	110.49	109.88
			H18-C16-C19	110.49	109.88
			C16-C19-H20	113.95	112.24
			C16-C19-H21	113.95	112.24
			C16-C19-S22	109.06	109.48
			H20-C19-H21	113.95	111.15
			H20-C19-S22	102.75	105.64
			H21-C19-S22	102.75	105.64
			C19-S22-O23	109.48	109.57
			C19-S22-O24	109.48	109.57
			C19-S22-Cl25	97.30	98.83
			O23-S22-O24	121.26	121.85
			O23-S22-Cl25	108.33	107.24
			O24-S22-Cl25	108.33	107.24

5. Non-linear Optical Properties (NLO)

Modern communication technology relies heavily on quantum chemistry, which predicts a molecule's non-linear optical properties for material design, signal processing, and optical links (Kumar et al., 2018). The growth of electronic device applications requires nonlinear optical (NLO) features. Changes in molecular optical characteristics, such as frequency, phase and amplitude in the presence of an electromagnetic field, give rise to the NLO features (Teotia et al., 2016). Recently, nonlinear optical (NLO) materials attracts because of their prospective uses in many industries, including laser technology and telecommunications (Aswathy et al., 2025). Numerous scholars (Annu et al., 2022; Kumar et al., 2022; Teotia et al., 2022; Yadav et al., 2022) have examined the mean polarisability <α>, anisotropy of the polarisability Δα, total first-order hyperpolarizability β_{total}, hyperpolarizability of first and second order, and dipole moment μ. These can be computed using the following formulas.

$$< \alpha >= \frac{(\alpha_{xx}+\beta_{yy}+\gamma_{zz})}{3} \quad (1)$$

$$\Delta\alpha = \left[\frac{1}{2}\left\{(\alpha_{yy}-\alpha_{zz})^2 + (\alpha_{xx}-\alpha_{yy})^2 + (\alpha_{zz}-\alpha_{xx})^2 + 6(\alpha_{xy}^2+\alpha_{zy}^2+\alpha_{xz}^2)\right\}\right]^{\frac{1}{2}} \quad (2)$$

$$\beta_{Total} = (\beta_x^2+\beta_y^2+\beta_z^2)^{\frac{1}{2}} \quad (3)$$

where, $\beta_x = (\beta_{xxx}+\beta_{xyy}+\beta_{xzz})$, $\beta_y = (\beta_{yyy}+\beta_{xxy}+\beta_{yzz})$, $\beta_z = (\beta_{zzz}+\beta_{xxz}+\beta_{yyz})$

$$< \gamma >= \frac{1}{5}(\gamma_{xxxx}+\gamma_{yyyy}+\gamma_{zzzz}+2\gamma_{xxyy}+2\gamma_{xxzz}+2\gamma_{yyzz}) \quad (4)$$

where, $\gamma_{xxyy} = \gamma_{yyxx} = \gamma_{xyyx} = \gamma_{yxxy}$; $\gamma_{xxzz} = \gamma_{zzxx} = \gamma_{xzzx} = \gamma_{zxxz}$; $\gamma_{zzyy} = \gamma_{yyzz} = \gamma_{yzzy} = \gamma_{zyyz}$

$$\mu = (\mu_x+\mu_y+\mu_z)^{\frac{1}{2}} \quad (5)$$

According to **Table 3**, the dipole moment, polarizabilities α, and hyperpolarizabilities β for the molecule (2-PESC) are computed with the B3LYP/6-311++G (d,p) and B3LYP/cc-pVDZ sets.

Table 3. Non-linear optical parameters of molecule 2-Phthalimidoethanesulfonyl chloride calculated at B3LYP/6-311++G(d,p) and B3LYP/cc-pVDZ sets.

Parameters	B3LYP/6-311++G(d, p)	B3LYP/cc-pVDZ
Molecular Polarizability (a.u.)		
α_{xx}	-116.906	-110.314
α_{xy}	-3.014	-0.566
α_{yy}	-114.041	-104.043
α_{xz}	0.000	0.000
α_{yz}	0.000	0.000
α_{zz}	-128.111	-120.916
Mean polarizability<α>	-119.692	-111.758
Anisotropic polarizabilityΔα	16.5	17.6
Hyperpolarizability (a.u)		
β_{xxx}	14.263	9.849
β_{xxy}	3.143	-17.752
β_{xyy}	-31.172	-34.605
β_{yyy}	271.003	161.066
β_{xxz}	0.000	0.000
β_{xyz}	0.000	0.000
β_{yyz}	0.000	0.000
β_{xzz}	-15.993	-12.064
β_{yzz}	24.999	8.855
β_{zzz}	0.000	0.000
β_{x}	-1.486	-1.659
β_{y}	9.889	6.946
β_{z}	0.000	0.000
β_{Total}	10.000 (0.0864×10^{-30} esu)	7.141 (0.0617×10^{-30} esu)
γ_{xxxx}	-611.319	-495.824
γ_{yyyy}	-7168.245	-6590.727
γ_{zzzz}	-1050.317	-965.585
γ_{xxxy}	10.583	27.764
γ_{xxxz}	0.000	0.000
γ_{yyyx}	-179.659	-94.745
γ_{yyyz}	0.000	0.000
γ_{zzzx}	0.000	0.000
γ_{zzzy}	0.000	0.000
γ_{xxyy}	-1469.217	-1310.719
γ_{xxzz}	-270.218	-238.741
γ_{yyzz}	-1391.782	-1292.390
γ_{xxyz}	0.000	0.000
γ_{yyxz}	0.000	0.000
γ_{zzxy}	-0.011	-0.610
Average second order hyperpolarizability <γ>	-3018.463	-2747.167

The highest negative value for the polarisability component α_{zz} is –128.111 a.u. at 6-311++G (d,p) core level. In the B3LYP/6-311++G(d,p) and B3LYP/cc-pVDZ basis sets, the computed value of β_{Total} is 10.000 a.u. and 7.141 a.u., respectively, while the maximum negative value of component β_{xyy} of first-order hyperpolarizability is -34.605 at the cc-pVDZ set and the maximum positive value of component $\beta_{yyy,}$ is 271.003 a.u. at 6-311++G (d,p) set. The component γ_{xxxy} of second-order hyperpolarizability has the maximum positive value of 27.764 a.u. at the cc-pVDZ basis level and the component γ_{yyyy} has the maximum negative value equal to -7168.245 a.u. at 6-311++G(d,p) set. The total value of second order hyperpolarizability <γ> is -3018.463 a.u. and -2747.167 a.u at 6-311++G (d,p) and cc-pVDZ core level, respectively. The various computed values in **Table 3** are marginally higher in the B3LYP/6-311++G(d,p) core basis set as compared to the B3LYP/cc-pVDZ set. Molecule (2-PESC) has a hyperpolarizability value of 0.0864×10^{-30} esu at the 6-311G++(d,p) set and 0.0617×10^{-30} esu at the cc-pVDZ set, whereas urea has a value of 0.1947×10^{-30} esu. The fact that these values are much lower than

those of the urea molecule suggests that the molecule (2-PESC) does not have good NLO properties. Due to the phthalimido group, the molecule exhibits some NLO features. Some known NLO chromophores are DAST and DR1. The thermal stability of NLO chromophores is low, electron delocalization performance is high and their π-system is long & rigid and they have high first order hyperpolarizabilities because of their effective internal charge transfer (ICT). The molecule 2-phthalimidoethanesulfonyl chloride has high reactivity with water and alcohol. It has high thermal stability and exhibits low electron delocalization performance, and its π-system is also short and broken. So, from the above discussion, it is concluded that the molecule 2-PESC is not a high performance NLO candidate compared to other NLO chromophores. The NLO strength of molecule 2-PESC is moderate.

6. Mulliken Charges

The Mulliken population analysis is used to estimate the partial atomic charges, or Mulliken charges. Here, the B3LYP/6-311++G(d,p) and B3LYP/cc-pVDZ core levels are used to evaluate mulliken charges. For the calculations, computational chemistry methods are used, namely those based on the linear arrangement of atomic orbitals, which are commonly used as variables in rectilinear regression algorithms. The positive and negative mulliken charges of the molecule (2-PESC) are shown in **Figure 2**.

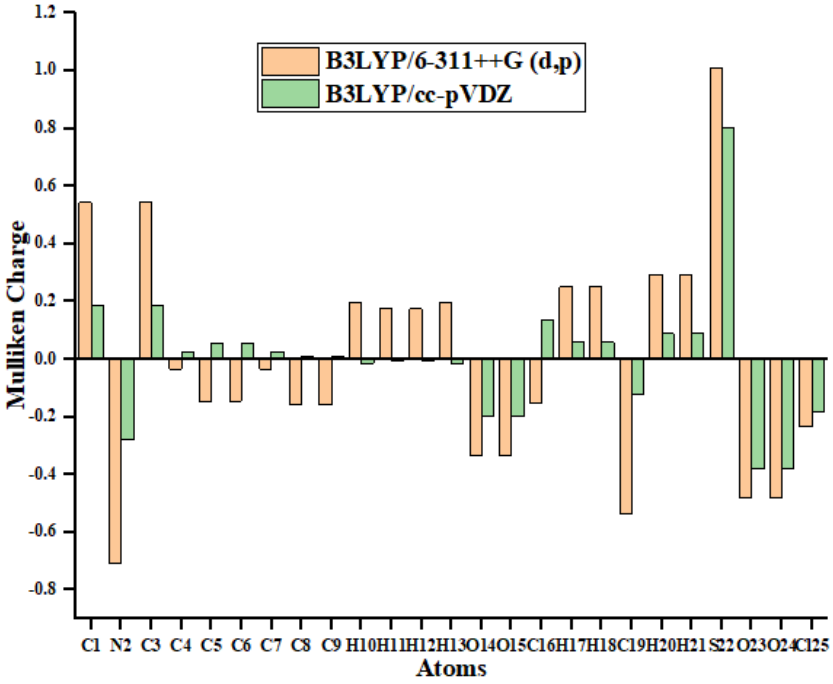

Figure 2. Mulliken charges of the molecule (2-PESC) computed by B3LYP /6-311++G(d,p) and B3LYP/cc-pVDZ sets [C-Carbon, N-Nitrogen, H-Hydrogen, O-Oxygen, S- Sulphur, Cl-Chlorine].

6.1 Charge Localization to Sulfonyl Chloride Group

The confinement of electric charge carriers (electrons or holes) to particular locations is known as charge localization. In the sulfonyl chloride group (-SO_2Cl), the sulphur atom is bonded to two electronegative atoms (oxygen atom and chlorine atom). According to **Figure 2**, the sulphur atom has the largest positive mulliken value (highest peak on the positive y axis), showing electron deficiency, and the oxygen and chlorine atoms have negative mulliken values (downward peaks towards y axis), indicating localised

electron density on the electronegative atom. Hence, one of the main sites of charge laocalization is a sulfonyl chloride group, particularly the sulfur atom, which functions as a strong electrophilic center.

6.2 Charge Localization to the Phthalimide Moiety

According to the mulliken graph, the carbonyl oxygens have significant negative charges as shown by the downward peaks in the **Figure 2**. They carry electron density due to the high electronegativity of oxygen atoms. The carbonyl carbons carry both positive and negative values, as shown in the mulliken graph. Carbon is regarded as a mildly electronegative atom. The imide nitrogen carries a significantly negative charge, as shown in the **Figure 2**. The phthalimide moiety acts as an electron-deficient system. So, the electron-withdrawing property of the phthalimide moiety has a significant impact on the charge localization.

7. Thermodynamic Functions

Using a Perl script, the thermodynamic properties of a molecule, i.e. heat capacity, entropy, and enthalpy are calculated in the temperature range from 100K to 1000K. **Figure 3** displays the plot of temperature variation with the computed thermodynamic functions and **Table 5** lists the relevant values. These computations are made at the B3LYP/cc-pVDZ basis set utilising DFT calculations. **Table 4** shows the calculated thermodynamic parameters at room temperature for both basis sets. The graph shows that as the temperature rises, the three thermodynamic parameters rise. Numerous scholars have examined these thermodynamic properties (Yadav et al., 2023).

Table 4. Thermodynamic parameters of the molecule (2-PESC) calculated at B3LYP/6-311++G(d,p) and B3LYP/cc-pVDZ sets.

Parameters	**B3LYP/ 6-311++G(d,p)**	**B3LYP/ cc-pVDZ**
Zero point vibrational energy(J/mol)	447929.2	454968.5
Rotational constant(GHz)	0.891	0.972
	0.160	0.166
	0.152	0.157
Thermal energy(kcal/mol)		
Total	117.210	117.797
Translational	0.889	0.889
Rotational	0.889	0.889
Vibrational	115.433	116.019
Specific heat(Cal/mol-k)		
Total	57.586	53.830
Translational	2.981	2.981
Rotational	2.981	2.981
Vibrational	51.624	47.869
Entropy(Cal/mol-k)		
Total	137.128	123.893
Translational	42.712	42.712
Rotational	33.959	33.807
Vibrational	60.456	47.375
Dipole moment(Debye)		
μ_x	-1.486	-1.659
μ_y	9.889	6.946
μ_z	0.000	0.000
Total	10.000	7.141

Table 5. Variation of thermodynamic functions at different temperatures using B3LYP/6-311++G(d,p) for 2-Phthalimidoethanesulfonyl chloride.

T (K)	S (J/mol.K)	Cp (J/mol.K)	ddH (kJ/mol)
100	382.938	120.652	8.060
150	438.475	154.941	14.966
200	487.477	187.165	23.522
250	532.675	219.076	33.679
298.15	573.855	249.254	44.957
300	575.400	250.392	45.420
350	616.266	280.280	58.694
400	655.532	308.049	73.412
450	693.300	333.339	89.458
500	729.620	356.084	106.704
550	764.530	376.413	125.026
600	798.075	394.550	144.308
650	830.307	410.751	164.448
700	861.288	425.261	185.355
750	891.081	438.304	206.950
800	919.750	450.073	229.164
850	947.361	460.730	251.939
900	973.974	470.413	275.221
950	999.648	479.237	298.966
1000	1024.437	487.301	323.132

where, [T] represents Temperature in Kelvin, [S] represents Entropy in J mol^{-1} K^{-1}, [Cp] represents Heat capacity at constant pressure in kJ mol^{-1} K^{-1} and [ddH] represents H (T)-H (0) (enthalpy content, in kJ mol^{-1}).

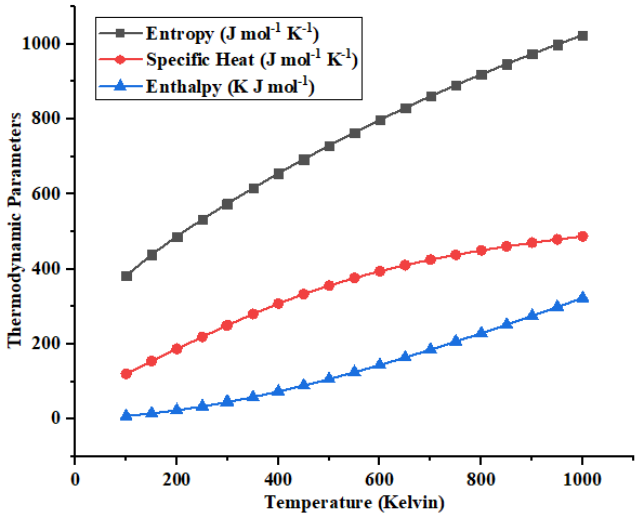

Figure 3. Variation of the thermodynamic functions with temperature of the molecule (2-PESC).

8. Natural Bond Orbital (NBO)

Using local eigenvectors of a single particle density matrix, the Natural Bond Orbital (NBO) facilitates the investigation of covalent effects and hybridization in polyatomic wave functions. Acceptor non-Lewis NBOs and donor Lewis NBOs, for which electron densities are employed, interact in NBO analysis using the second-order perturbation theory (Reeda & Jothy, 2023; Aygün et al., 2024). Understanding

intramolecular and intermolecular interactions may be enhanced by the proper explanation provided by the NBO analysis, which is the relationship between filled and virtual orbital spaces. The interaction between the filled and anti-bonding orbitals, which may also be employed as a measure of delocalisation, represents the molecule's departure from the Lewis structure. The perturbation interaction of second order ($E^{(2)}$) energy provides a quantitative explanation of this non-covalent bonding–antibonding interaction (Foster & Weinhold, 1980; Reed & Weinhold, 1983; Reed et al., 1985; Reed & Weinhold, 1985). Numerous additional pertinent details, including directionality, partial charges, and hybridization have been examined in the NBO results (Weinhold, 2001; Weinholdet al., 2005).

Table 6 displays the difference of energy between donor (i) & acceptor (j) NBO orbitals, the stabilization energy, the Fock matrix element between i and j NBO orbitals, and the occupancy of donor & acceptor NBOs of the 2-PESC molecule. When the stabilization energy is high, the interaction between the donor and acceptor NBO is the largest. The largest estimated stabilization energy for the lone pair contact, which corresponds to the σ*(1) S22-Cl25 interaction for LP (3) O24, is 75.13 kcal/mol. The interaction between σ*(1) S22–Cl25 and LP (3) O23 is responsible for the second largest stabilization energy, which is 75.11 kcal/mol.

Table 6. NBO computation of the molecule (2-PESC) computed at B3LYP/cc-pVDZ set.

Donor NBO(i)	ED/e	Energy E(i)	Acceptor NBO(j)	Energy E(j)	E(2)[a] kcal/mol	E(j)-E(i)[b] (a.u.)	F(i,j)[c] (a.u.)
σ (1) Cl – N2	1.978	-0.764	σ*(1) N2 - C16	1.066	0.59	1.83	0.030
			σ*(1) C3 – O15	0.836	0.96	1.60	0.035
			σ*(1) C7 - C8	0.286	0.98	1.05	0.029
			σ*(1) C16 - H17	0.476	3.65	1.24	0.060
			σ*(1) C16 - C19	0.566	2.52	1.33	0.052
σ (1) C1 – C8	1.971	-0.669	σ*(1) N2 - C16	0.292	2.35	0.96	0.042
			σ*(1) C3 - O15	0.472	0.55	1.14	0.023
			σ*(1) C4 - C9	0.562	5.08	1.23	0.071
			σ*(1) C6 - C7	0.532	2.01	1.20	0.044
			σ*(1) C7 - C8	0.562	2.17	1.23	0.046
			σ*(1) C8 - C9	0.592	1.93	1.26	0.044
σ (1) C1- O14	1.996	-1.054	σ*(1) C1 - C8	0.366	0.76	1.42	0.030
			σ*(1) N2 - C3	0.286	0.88	1.34	0.031
			σ*(1) C8 - C9	0.596	0.69	1.65	0.030
σ (2) C1 – O14	1.976	-0.397	σ*(2) C8 - C9	0.013	3.73	0.41	0.039
σ (1) N2 – C3	1.978	-0.764	σ*(1) C1 - O14	0.476	3.65	1.24	0.060
			σ*(1) N2 - C16	0.286	0.98	1.05	0.029
			σ*(1) C4 - C9	0.566	2.52	1.33	0.052
			σ*(1) C16 - H18	0.466	0.61	1.23	0.025
			σ*(1) C16 - C19	0.316	0.69	1.08	0.024
σ (1) N2 – C16	1.971	-0.759	σ*(1) C1 - N2	0.281	0.76	1.04	0.026
			σ*(1) C1 – C8	0.361	1.33	1.12	0.035
			σ*(2) C1 - O14	-0.039	0.81	0.72	0.023
			σ*(1) N2 - C3	0.281	0.76	1.04	0.026
			σ*(1) C3 - C9	0.361	1.33	1.12	0.035
			σ*(2) C3 - O15	-0.039	0.81	0.72	0.023
			σ*(1) C19 - S22	0.111	2.53	0.87	0.043
σ (1) C3 – C9	1.971	-0.669	σ*(1) C1 – O14	0.472	0.55	1.14	0.023
			σ*(1) N2 - C16	0.292	2.35	0.96	0.042
			σ*(1) C4 - C5	0.532	2.01	1.20	0.044
			σ*(1) C4 - C9	0.562	2.17	1.23	0.046
			σ*(1) C7 - C8	0.562	5.08	1.23	0.071
			σ*(1) C8 - C9	0.592	1.93	1.26	0.044
σ (1) C3 – O15	1.996	-1.054	σ*(1) C1 - N2	0.286	0.88	1.34	0.031
			σ*(1) C3 - C9	0.366	0.76	1.42	0.030
			σ*(1) C8 - C9	0.596	0.69	1.65	0.030

Table 6 continued…

σ (2) C3 – O15	1.976	-0.397	σ*(2) C8 - C9	0.013	3.73	0.41	0.039
σ (1) C4 – C5	1.977	-0.717	σ*(1) C3 - C9	0.363	5.69	1.08	0.071
			σ*(1) C4 – C9	0.563	3.09	1.28	0.056
			σ*(1) C4 - H10	0.463	1.19	1.18	0.034
			σ*(1) C5 - C6	0.513	1.91	1.23	0.043
			σ*(1) C5 - H11	0.463	1.03	1.18	0.031
			σ*(1) C6 - H12	0.463	2.26	1.18	0.046
σ (2) C4 – C5	1.631	-0.282	σ*(2) C6 – C7	-0.002	18.82	0.28	0.066
			σ*(2) C8 – C9	0.008	22.32	0.29	0.073
σ (1) C4 – C9	1.974	-0.740	σ*(1) C1 – C8	0.360	2.59	1.10	0.048
			σ*(1) N2 – C3	0.280	0.74	1.02	0.025
			σ*(1) C3 - C9	0.360	2.59	1.10	0.048
			σ*(1) C4 - C5	0.530	2.22	1.27	0.048
			σ*(1) C4 - H10	0.460	1.44	1.20	0.037
			σ*(1) C5 - H11	0.470	2.30	1.21	0.047
			σ*(1) C8 - C9	0.590	5.64	1.33	0.077
σ (1) C4 – H10	1.981	-0.555	σ*(1) C4 – C5	0.535	0.65	1.09	0.024
			σ*(1) C4 – C9	0.565	1.01	1.12	0.030
			σ*(1) C5 - C6	0.515	3.77	1.07	0.57
			σ*(1) C8 - C9	0.595	4.90	1.15	0.67
σ (1) C5 – C6	1.981	-0.715	σ*(1) C4 – C5	0.535	2.00	1.25	0.045
			σ*(1) C4 - H10	0.465	2.48	1.18	0.048
			σ*(1) C5 - H11	0.465	1.04	1.18	0.031
			σ*(1) C6 - C7	0.535	2.00	1.25	0.045
			σ*(1) C6 - H12	0.465	1.04	1.18	0.031
			σ*(1) C7 - H13	0.465	2.48	1.18	0.048
σ (1) C5 – H11	1.982	-0.557	σ*(1) C4 – C5	0.533	0.53	1.09	0.021
			σ*(1) C4 - C9	0.563	3.82	1.12	0.059
			σ*(1) C5 - C6	0.513	0.52	1.07	0.021
			σ*(1) C6 - C7	0.533	3.86	1.09	0.058
σ (1) C6 – C7	1.977	-0.717	σ*(1) C1 – C8	0.363	5.69	1.08	0.071
			σ*(1) C5 – C6	0.513	1.91	1.23	0.043
			σ*(1) C5 – H11	0.463	2.26	1.18	0.046
			σ*(1) C6 – H12	0.463	1.03	1.18	0.031
			σ*(1) C7 - C8	0.563	3.09	1.28	0.056
			σ*(1) C7 - H13	0.463	1.19	1.18	0.034
σ (2) C6 – C7	1.631	-0.282	σ*(2) C4 – C5	-0.002	18.82	0.28	0.066
			σ*(2) C8 – C9	0.008	22.32	0.29	0.073
σ (1) C6 – H12	1.982	-0.557	σ*(1) C4 – C5	0.533	3.86	1.09	0.058
			σ*(1) C5 – C6	0.513	0.52	1.07	0.021
			σ*(1) C6 – C7	0.533	0.53	1.09	0.021
			σ*(1) C7 – C8	0.563	3.82	1.12	0.059
σ (1) C7 – C8	1.974	-0.740	σ*(1) C1 – N2	0.280	0.74	1.02	0.025
			σ*(1) C1 – C8	0.360	2.59	1.10	0.048
			σ*(1) C3 - C9	0.360	2.59	1.10	0.048
			σ*(1) C6 – C7	0.530	2.22	1.27	0.048
			σ*(1) C6 - H12	0.470	2.30	1.21	0.047
			σ*(1) C7 - H13	0.460	1.44	1.20	0.037
			σ*(1) C8 - C9	0.590	5.64	1.33	0.077
σ (1) C7 – H13	1.981	-0.555	σ*(1) C5 - C6	0.515	3.77	1.07	0.057
			σ*(1) C6 - C7	0.535	0.65	1.09	0.024
			σ*(1) C7 - C8	0.565	1.01	1.12	0.030
			σ*(1) C8 - C9	0.595	4.90	1.15	0.067
σ (1) C8 – C9	1.964	-0.739	σ*(1) C1 – C8	0.361	1.25	1.10	0.033
			σ*(1) C1 – O14	0.471	2.95	1.21	0.054
			σ*(1) C3 – C9	0.361	1.25	1.10	0.033
			σ*(1) C3 – O15	0.471	2.95	1.21	0.054
			σ*(1) C4 – C9	0.571	4.90	1.31	0.072
			σ*(1) C4 - H10	0.461	2.54	1.20	0.050
			σ*(1) C7 - C8	0.571	4.90	1.31	0.072

Table 6 continued…

			σ*(1) C7 - H13	0.461	2.54	1.20	0.050
σ (2) C8 – C9	1.634	-0.295	σ*(2) C1 – O14	-0.035	18.38	0.26	0.064
			σ*(2) C3 – O15	-0.035	18.38	0.26	0.064
			σ*(2) C4 – C5	-0.005	18.62	0.29	0.067
			σ*(2) C6 - C7	-0.005	18.62	0.29	0.067
σ (1) C16 – H17	1.982	-0.552	σ*(1) C1 – N2	0.278	1.86	0.83	0.036
			σ*(1) C19 – H20	0.448	2.70	1.00	0.046
σ (1) C16 – H18	1.982	-0.552	σ*(1) N2 – C3	0.278	1.86	0.83	0.036
			σ*(1) C19 – H21	0.448	2.71	1.00	0.046
σ (1) C16 – C19	1.976	-0.664	σ*(1) C1 – N2	0.286	1.11	0.95	0.029
			σ*(1) N2 – C3	0.286	1.11	0.95	0.029
			σ*(1) C16 - H17	0.466	0.51	1.13	0.022
			σ*(1) C16 - H18	0.466	0.51	1.13	0.022
			σ*(1) C19 - H20	0.446	0.70	1.11	0.025
			σ*(1) C19 - H21	0.446	0.70	1.11	0.025
			σ*(1) S22 - Cl25	-0.214	1.80	0.45	0.031
σ (1) C19 – H20	1.975	-0.570	σ*(1) C16 – H17	0.460	2.72	1.03	0.047
			σ*(1) C16 – C19	0.320	0.50	0.89	0.019
			σ*(1) S22 – O24	0.160	2.78	0.73	0.042
σ (1) C19 – H21	1.975	-0.570	σ*(1) C16 – H18	0.460	2.72	1.03	0.047
			σ*(1) C16 – C19	0.320	0.50	0.89	0.019
			σ*(1) S22 – O23	0.160	2.78	0.73	0.042
σ (1) C19– S22	1.957	-0.766	σ*(1) N2 – C16	0.284	2.85	1.05	0.049
			σ*(1) C19 – S22	2.114	0.62	2.88	0.021
			σ*(1) S22 – O23	0.154	4.02	0.92	0.056
			σ*(1) S22 – O24	0.154	4.02	0.92	0.056
			σ*(1) S22 – Cl25	-0.216	1.92	0.55	0.035
σ (1) S22– O23	1.966	-0.956	σ*(1) C19 – H21	0.454	0.64	1.41	0.027
			σ*(1) C19 – S22	0.114	2.16	1.07	0.044
			σ*(1) S22 – O23	0.154	1.05	1.11	0.031
			σ*(1) S22 – O24	0.154	4.36	1.11	0.064
σ (1) S22 – O24	1.966	-0.956	σ*(1) C19 – H20	0.454	0.64	1.41	0.027
			σ*(1) C19 – S22	0.114	2.16	1.07	0.044
			σ*(1) S22 – O23	0.154	4.37	1.11	0.064
			σ*(1) S22 – O24	0.154	1.04	1.11	0.031
σ (1) S22 – Cl25	1.904	-0.430	σ*(1) C16 – C19	0.320	4.24	0.75	0.051
			σ*(1) C19 – S22	0.110	4.11	0.54	0.043
			σ*(1) S22 – O23	0.160	12.63	0.59	0.078
			σ*(1) S22 – O24	0.160	12.63	0.59	0.078
			σ*(1) S22 – Cl25	-0.220	6.75	0.21	0.040
LP (1) N2	1.710	-0.356	σ*(2) C1 – O14	-0.036	25.45	0.32	0.082
			σ*(2) C3 – O15	-0.036	25.45	0.32	0.082
			σ*(1) C16 – H17	0.464	1.44	0.82	0.033
			σ*(1) C16 – H18	0.464	1.43	0.82	0.033
			σ*(1) C16 – C19	0.324	3.06	0.68	0.043
			σ*(1) C19 – S22	0.114	1.52	0.47	0.025
LP (1) O14	1.974	-0.729	σ*(1) C1 – N2	0.281	1.92	1.01	0.040
			σ*(1) C1 – C8	0.361	2.81	1.09	0.050
LP (2) O14	1.852	-0.289	σ*(1) C1 – N2	0.281	27.73	0.57	0.114
			σ*(1) C1 – C8	0.361	16.24	0.65	0.094
LP (1) O15	1.974	-0.729	σ*(1) N2 – C3	0.281	1.92	1.01	0.040
			σ*(1) C3 – C9	0.361	2.81	1.09	0.050
LP (2) O15	1.852	-0.289	σ*(1) N2 – C3	0.281	27.73	0.57	0.114
			σ*(1) C3 – C9	0.361	16.24	0.65	0.094
LP (1) O23	1.981	-0.842	σ*(1) C19 – S22	0.118	0.89	0.96	0.027
			σ*(1) S22 – O24	0.158	0.57	1.00	0.022
			σ*(1) S22 – Cl25	-0.212	2.59	0.63	0.044
LP (2) O23	1.830	-0.337	σ*(1) C19 – H21	0.453	0.51	0.79	0.019
			σ*(1) C19 – S22	0.113	8.36	0.45	0.055
			σ*(1) S22 – O24	0.153	20.43	0.49	0.090

Table 6 continued…

			σ*(1) S22 – Cl25	-0.217	6.11	0.12	0.028
LP (3) O23	1.644	-0.390	σ*(1) C19 – S22	0.110	5.26	0.50	0.049
			σ*(1) S22 – O23	0.160	12.16	0.55	0.077
			σ*(1) S22 – O24	0.160	0.76	0.55	0.019
			σ*(1) S22 – Cl25	-0.220	75.11	0.17	0.111
LP (1) O24	1.981	-0.842	σ*(1) C19 – S22	0.118	0.89	0.96	0.027
			σ*(1) S22 – O23	0.158	0.57	1.00	0.022
			σ*(1) S22 – Cl25	-0.212	2.59	0.63	0.044
LP (2) O24	1.830	-0.337	σ*(1) C19 - H20	0.453	0.51	0.79	0.019
			σ*(1) C19 – S22	0.113	8.37	0.45	0.055
			σ*(1) S22 – O23	0.153	20.43	0.49	0.090
			σ*(1) S22 – Cl25	-0.217	6.10	0.12	0.028
LP (3) O24	1.644	-0.390	σ*(1) C19 – S22	0.110	5.25	0.50	0.049
			σ*(1) S22 – O23	0.160	0.76	0.55	0.019
			σ*(1) S22 – O24	0.160	12.17	0.55	0.077
			σ*(1) S22 – Cl25	-0.220	75.13	0.17	0.111
LP (2) Cl25	1.983	-0.306	σ*(1) S22 – O23	0.154	1.06	0.46	0.021
			σ*(1) S22 – O24	0.154	1.06	0.46	0.021
LP (3) Cl25	1.978	-0.414	σ*(1) C16 – C19	0.424	4.27	0.73	0.050

where, [E (2) represents stabilization energy; E (j)-E (i) represents Energy difference of donor (i) & acceptor (j) NBO orbitals; F (i,j) represents Fock matrix element between orbitals of i & j NBO and ED/e represents occupancy].

9. Vibrational Interpretation

This work uses both theoretical and experimental methods to determine the vibrational frequencies using the FT-IR and FT-Raman studies. Density functional theory at B3LYP/6-311++G (d,p) and B3LYP/cc-pVDZ core levels is used for the theoretical calculations of the optimised molecule. **Figures 4** and **5** show the theoretical and observed FTIR and Raman spectra, respectively, which are used to determine vibrational frequencies.

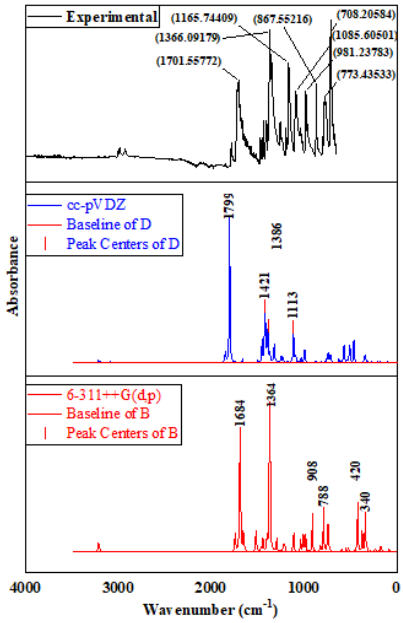

Figure 4. Experimental and computed FTIR spectra of the molecule (2-PESC).

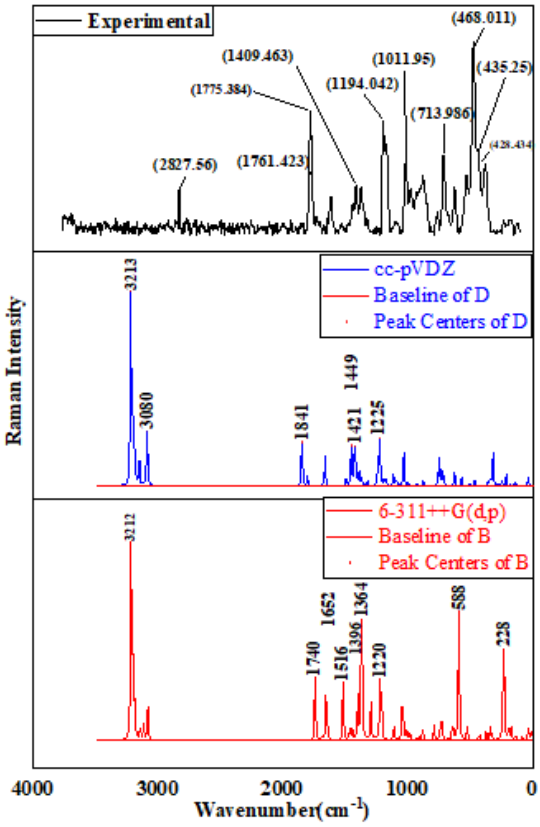

Figure 5. Experimental and computed Raman spectra of the molecule (2-PESC).

When compared to experimental values, the theoretical FT-IR/FT-Raman wavenumbers are overestimated, and several scaling factors are applied to bring computational and experimental wavenumbers into alignment. The scaling factor 'C' is formulated as:

$$C = \frac{\sum(r_i \times w_i)}{\sum w_i^2} \quad (6)$$

where, the measured fundamental frequency is denoted by r_i and the theoretical frequency by w_i.

In order to compute the scaling factors for the unscaled harmonic wavenumbers and perform density functional theory calculations of the (2-PESC) molecule, two large basis levels, 6–311++G(d,p) and cc-pVDZ, were taken into consideration. Using the scaling factors, the scaled wavenumbers for the various possible modes of vibration at the B3LYP/6–311++G(d,p) and B3LYP/cc-pVDZ core levels were calculated in this work. **Table 7** provides the scaling factor for several potential modes of vibration. Torsion, bending, and stretching are the three general categories into which the potential vibrational modes fall. At 6–311++G(d,p) and cc-pVDZ core levels, the scaling factors for stretching, bending (in-plane), torsion, and bending(out-of-plane) vibrations are 0.961, 0.968, 0.977, 0.964 and 0.952, 0.955, 0.979, 0.935 respectively. The scaled wavenumbers in both sets are computed using these scaling factors. The VEDA algorithm (Jamróz, 2013) computes the detailed vibrational assignment contribution of different vibrational modes for both basis sets. **Table 8** displays the vibrational assignments and experimental, scaled, and unscaled wavenumbers for the (2-PESC) molecule. In the molecule 2-

phthalimidoethanesulfonyl chloride, there are three main structural components: phthalimido group (C=O), sulfonyl chloride group (S=O) and an ethane linker (C-H).

Table 7. Scaling factors used to calculate scaled computational wavenumbers for B3LYP/cc-pVDZ and B3LYP/6-311++G (d,p) sets.

vibrational assignment	B3LYP/6-311++G(d,p) scaling factor	B3LYP/cc-pVDZ scaling factor	serial numbers
νC–H	0.961	0.952	1-8
νO–C	0.961	0.952	9-10
νC–C	0.961	0.952	11-12, 14, 19, 24-26, 29, 31, 34
νN–C	0.961	0.952	20, 33, 34, 48
νS–O	0.961	0.952	36, 37, 39
νS–C	0.961	0.952	47, 49
νCl–S	0.961	0.952	52, 58
β (in-plane bending)	0.968	0.955	12-16, 18, 21, 23-29, 37, 40, 43-44, 46-48, 53-57, 59-62, 64-65, 67
τ(torsion)	0.977	0.979	17-18, 22, 27-28, 30, 32, 38, 40, 45, 50-51, 60-66, 68-69
γ (out of plane bending)	0.964	0.935	38, 41-42, 45, 50, 52, 55, 57-59, 62-64, 67

9.1 C–H Vibrations

The aromatic C–H stretching oscillations are found in the 3100–3000 cm^{-1} region, while the C–H bending modes are found in the 1000–680 cm^{-1} range, according to Colthup et al. (2012). In the Phthalimide derivatives, the νC–H vibrations occur between 3300 cm^{-1} and 3100 cm^{-1} (Leela et al., 2015).

In the (2-PESC) molecule, the aromatic C-H stretching oscillations are found at 2982 & 2924 cm^{-1} in the FT-IR spectrum and at 2826 cm^{-1} in the FT-Raman spectrum. The in-plane bending modes for C-H oscillations are found at 1467 cm^{-1} in the FT-IR region. The βH-C-C oscillations are found at 1170 & 773 cm^{-1} in the FT-IR region and at 1193 & 1012 cm^{-1} in the FT-Raman region.

9.2 C–C Vibrations

According to Colthup et al. (2012), the C–C aromatic stretching vibrations are found in the region of 1600–1450 cm^{-1} and aliphatic C-C stretching appears in the region of 1300–900 cm^{-1}. In the (2-PESC) molecule, the FT-IR spectrum exhibits C-C stretching vibrations at wavenumbers 1170, 1166, 1033, and 981 cm^{-1}, while the FT-Raman spectrum shows the same vibrations at wavenumbers 1610, 1514, 1369, 1193, and 980 cm^{-1}. The C-C bending modes can be seen in the FT-IR spectrum at wavenumbers 1086, 868, and 710 cm^{-1}, and in the FT-Raman spectrum at wavenumbers 1514, 1090, 876, 711, and 527 cm^{-1}. In the FT-Raman spectrum, the C-C torsion vibrational modes are detected at a wavenumber 173 cm^{-1}. The γC-C-C-C bending mode is found at wavenumber 761cm^{-1} in the FT-Raman spectrum.

9.3 C–N Vibrations

In this molecule (2-PESC), at wavenumbers 1346, 980, and 527 cm^{-1} in the FT-Raman spectrum and at 1365 and 981 cm^{-1} in the FT-IR spectrum, the C-N stretching beats are observed. The βC-N-C oscillations are detected at wavenumber 1365 cm^{-1} in the FT-IR spectrum and wavenumbers 1346 and 621 cm^{-1} in the FT-Raman spectrum. The βN-C-C oscillations are detected at wavenumber 868 cm^{-1} in the FT-IR spectrum and at 876 and 527 cm^{-1} in the FT-Raman spectrum. The βC-C-N vibration is observed in the FT-Raman spectrum at wavenumber 173 cm^{-1}. Both the τN-C-C-C and τC-N-C-C vibrations were detected at wavenumbers 173 cm^{-1} & 123 cm^{-1}, respectively, in the FT-Raman spectrum. The FT-IR and FT-Raman spectra show the τH-C-N-C vibration at wavenumbers 1403 cm^{-1} and 1411 cm^{-1}, respectively.

The FT-IR spectrum shows the H-C-C-N oscillations at wavenumbers 1254, 1086, and 773 cm^{-1}, while the FT-Raman spectrum shows them at wavenumber 1090 cm^{-1}.

9.4 C=O Vibrations

In this molecule (2-PESC) of phthalimide derivative, the C=O groups located in the phthalimide moiety are known as carbonyl carbons. The reactivity of the entire molecule may be impacted by the carbonyl carbons due to electron-withdrawing properties. The C=O stretching shaking modes are detected at wavenumber 1702 cm^{-1} in the FT-IR spectrum & at 1772 cm^{-1} in the FT-Raman spectrum.

Table 8. Computed and observed vibrational assignments of molecule (2-PESC) at B3LYP/cc-pVDZ and B3LYP/6-311++G(d, p) core levels.

S. No.	Observed Wavenumber (cm^{-1}) FT-IR	RAMAN	B3LYP/ 6-311++G(d,p) Calculated wavenumber Unscaled	Scaled	B3LYP/ cc-pVDZ Calculated wavenumber Unscaled	Scaled	Probable Assignments (>10%)
1.			3212	3089	3213	3059	νC_4-H_{10}(25)+ νC_5-H_{11}(25)+ νC_6-H_{12}(25)+ νC_7-H_{13}(25)
2.			3205	3081	3210	3057	νC_4-H_{10}(43)+ νC_7-H_{13}(43)
3.			3204	3080	3198	3045	νC_{19}-H_{20}(49)+ νC_{19}-H_{21}(49)
4.			3195	3071	3185	3033	νC_4-H_{10}(25)+ νC_5-H_{11}(25)+ νC_6-H_{12}(25)+ νC_7-H_{13}(25)
5.			3182	3059	3172	3020	νC_5-H_{11}(43)+ νC_6-H_{12}(43)
6.			3137	3016	3144	2994	νC_{16}-H_{17}(49)+ νC_{16}-H_{18}(49)
7.	2982(vw)		3110	2990	3092	2944	νC_{19}-H_{20}(49)+ νC_{19}-H_{21}(49)
8.	2924(vw)	2826(w)	3077	2958	3082	2935	νC_{16}-H_{17}(49)+ νC_{16}-H_{18}(49)
9.	1702(s)	1772(vs)	1738	1671	1844	1756	νO_4-C_1(36)+ νO_{15}-C_3(36)+ νO_4-C_{15}(86)+ βC_3-N_2-C_1(11)
10.			1687	1622	1799	1713	νO_{14}-C_1(39)+ νO_{15}-C_3(39)
11.		1610(w)	1649	1585	1660	1581	νC_8-C_7(27)+ νC_9-C_4(27)
12.		1514(vw)	1641	1577	1656	1577	νC_8-C_7(13)+ νC_9-C_4(13)+ νC_6-C_5(25) + βC_9-C_4-C_5(10)+ βC_8-C_7-C_6(11)
13.			1515	1466	1495	1428	βH_{17}-C_{16}-H_{18}(88)
14.	1467(vw)		1513	1464	1492	1426	νC_7-C_6(10)+ βH_{11}-C_5-C_6(33)+ βH_{12}-C_6-H_7(29)
15.			1504	1456	1450	1385	βH_{10}-C_4-C_5(21)+ βH_{13}-C_7-C_6(21)
16.			1463	1416	1426	1363	βH_{21}-C_{19}-H_{20}(93)
17.	1403(w)	1411(w)	1441	1408	1418	1388	τH_{17}-C_{16}-N_2-C_1(43) +τH_{18}-C_{16}-N_2-C_1(25)
18.			1398	1353	1399	1337	βH_{18}-C_{16}-C_{19}(59)+ τH_{17}-C_{16}-N_2-C_1(17) +τH_{18}-C_{16}-N_2-C_1(15)
19.		1369(w)	1397	1343	1385	1319	νC_8-C_7(17) + νC_9-C_4(17) + νC_6-C_5(11)
20.	1365(vs)	1346(vw)	1367	1314	1367	1302	νN_2-C_3(11) + νN_2-C_{16}(29) + βC_3-N_2-C_1(25)
21.			1340	1297	1319	1260	βH_{10}-C_4-C_5(26)+ βH_{13}-C_7-C_6(26) + βC_3-N_2-C_1(25)
22.	1254(vw)		1292	1263	1298	1271	τH_{20}-C_{19}-C_{16}-N_2(46) +τH_{21}-C_{19}-C_{16}-N_2(42)
23.			1265	1224	1243	1188	βH_{18}-C_{16}-C_{19}(11) +βH_{20}-C_{19}-C_{16}(47)
24.			1221	1174	1238	1179	νC_5-C_4(18)+ νC_7-C_6(18)+ νC_1-C_8(14)+βH_{11}-C_5-C_6(16)+ βH_{12}-C_6-C_7(15)
25.	1170(vw)	1193(vs)	1208	1169	1222	1168	νC_6-C_5(10)+ νC_1-C_8(11)+ βH_{10}-C_4-C_5(14)+ βH_{11}-C_5-C_6(14)+ βH_{12}-C_6-C_7(14)+ βH_{13}-C_7-C_6(14)
26.	1166(s)		1207	1160	1187	1130	νC_5-C_4(14)+ νC_7-C_6(12)+ βC_9-C_4-C_5(13)
27.			1120	1094	1170	1146	βC_9-C_4-C_5(14)+ τH_{21}-C_{19}-C_{16}-N_2(17)
28.	1086(s)	1090(vw)	1108	1083	1111	1088	βC_9-C_4-C_5(10)+ τH_{21}-C_{19}-C_{16}-N_2(17)
29.		1012(s)	1044	1004	1096	1044	νC_5-C_4(12)+ νC_6-C_5(24)+ νC_7-C_6(12)+ βH_{10}-C_4-C_5(10)+ βH_{13}-C_7-C_6(10)
30.			1044	1020	1089	1066	τH_{11}-C_5-C_4-C_9(23)+τH_{12}-C_6-C_7-C_8(23)+τC_8-C_7-C_6-C_5(13)+ τC_9-C_4-C_5-C_6(11)+ τC_7-C_6-C_5-C_4(16)
31.	1033(w)		1034	994	1036	986	νC_{19}-C_{16}(78)
32.			1011	988	1029	1007	τH_{10}-C_4-C_9-C_8(31)+ τH_{11}-C_5-C_4-C_9(12)+ τH_{12}-C_6-C_7-C_8(12)+ τH_{13}-C_7-C_8-C_9(31)
33.			1005	966	1024	975	νN_2-C_1(21)+ νN_2-C_3(25)

Table 8 continued…

34.	**981(s)**	**980(w)**	**981**	**943**	**994**	**946**	**νC_6-C_5(10)+ νN_2-C_{16}(31)**
35.			933	912	990	969	τH_{10}-C_4-C_9-C_8(29)+ τH_{11}-C_5-C_4-C_9(15)+ τH_{12}-C_6-C_7-C_8(15)+ τH_{13}-C_7-C_8-C_9(29)
36.			909	874	988	941	νS_{22}-O_{23}(32)+ νS_{22}-O_{24}(32)
37.	868(w)	876(s)	879	851	921	880	νS_{22}-O_{23}(11)+ νS_{22}-O_{24}(11)+ βC_6-C_5-C_4(12)+ βN_2-C_1-C_8(11)
38.			821	802	876	858	τH_{11}-C_5-C_4-C_9(28)+ τH_{12}-C_6-C_7-C_8(28)+γO_{15}-N_2-C_9-C_3(10)+ γO_{14}-N_2-C_8-C_1(10)
39.			788	758	818	779	νS_{22}-O_{23}(42)+ νS_{22}-O_{24}(42)
40.	773(w)		784	759	812	776	βH_{20}-C_{19}-C_{16}(20)+τH_{20}-C_{19}-C_{16}-N_2(14)
41.		761(vw)	775	747	769	719	γO_{15}-N_2-C_9-C_3(14)+ γO_{14}-N_2-C_8-C_1(14)+ γC_1-C_7-C_9-C_8(20)
42.			742	715	748	700	γO_{15}-N_2-C_9-C_3(19)+ γO_{14}-N_2-C_8-C_1(19)
43.	710(vs)	711(s)	728	705	728	696	βC_6-C_5-C_4(14)+ βC_7-C_6-C_5(16)
44.			714	691	709	677	βO_{14}-C_1-C_8(23)+ βO_{15}-C_3-C_9(23)+ βC_6-C_5-C_4(11)+ βC_7-C_6-C_5(11)
45.			677	662	700	685	τC_8-C_7-C_6-C_5(20)+ τC_9-C_4-C_5-C_6(17)+ τC_7-C_6-C_5-C_4(13)+ γO_{15}-N_2-C_9-C_3(14)+ γO_{14}-N_2-C_8-C_1(14)
46.		621(w)	640	619	687	656	βC_3-N_2-C_1(25)+ βC_{19}-C_{16}-N_2(15)+ βS_{22}-C_{19}-C_{16}(11)
47.			590	567	622	592	νS_{22}-C_{19}(20)+ βC_3-N_2-C_1(17)
48.		527(w)	546	528	570	545	νN_2-C_1(10)+ βC_7-C_6-C_5(14)+ βN_2-C_1-C_8(14)+ βC_1-C_8-C_9(21)
49.		469(vs)	522	502	535	509	νS_{22}-C_{19}(32)
50.			463	452	507	496	τC_9-C_4-C_5-C_6(17)+ τC_7-C_6-C_5-C_4(13)+ γO_{15}-N_2-C_9-C_3(14)+ γO_{14}-N_2-C_8-C_1(14)
51.			432	422	475	465	τH_{10}-C_4-C_9-C_8(10)+ τH_{13}-C_7-C_8-C_9(10)+ τC_8-C_7-C_6-C_5(11)+ τC_9-C_4-C_5-C_6(30)
52.		378(w)	421	406	462	432	νCl_{25}-S_{22}(27)+γO_{24}-C_{19}-O_{23}-S_{22}(32)
53.			372	360	424	405	βC_{19}-C_{16}-N_2(13)+ βO_{24}-S_{22}-O_{23}(35)
54.			339	328	355	339	βO_{14}-C_1-C_8(22)+ βO_{15}-C_3-C_9(22)
55.			323	313	340	325	βO_{24}-S_{22}-C_{23}(32)+ βS_{22}-C_{19}-C_{16}(10)+ γC_{16}-C_1-C_3-N_2(20)
56.			280	271	331	316	βC_{16}-N_2-C_3(47)
57.			246	238	316	227	βC_1-C_8-C_9(21)+ γO_{23}-C_{19}-Cl_{25}-S_{22}(14)
58.		228(vw)	231	222	272	259	νCl_{25}-S_{22}(62)+γO_{24}-C_{19}-O_{23}-S_{22}(23)
59.			223	215	246	230	βC_{16}-N_2-C_3(16)+ γO_{23}-C_{19}-Cl_{25}-S_{22}(54)
60.		173(vw)	191	187	232	227	βC_{19}-C_{16}-N_2(11)+ βCl_{25}-S_{22}-C_{19}(14)+ τC_8-C_7-C_6-C_5(11)+ τN_2-C_1-C_8-C_7(31)
61.			172	166	211	202	βO_{23}-S_{22}-Cl_{25}(79)
62.			169	165	177	173	βCl_{25}-S_{22}-C_{19}(15)+ τC_3-N_2-C_1-C_8(34)+ γO_{15}-N_2-C_9-C_3(10)+ γO_{14}-N_2-C_8-C_1(10)
63.			142	139	142	139	τC_7-C_6-C_5-C_4(22)+ τN_2-C_1-C_8-C_7(31)+ γC_1-C_7-C_9-C_8(15)
64.		123(vw)	129	125	130	124	νS_{22}-C_{19}(20)+ βS_{22}-C_{19}-C_{16}(21)+τC_3-N_2-C_1-C_8(12)+ γO_{24}-C_{19}-O_{23}-S_{22}(10)
65.			84	81	100	96	βCl_{25}-S_{22}-C_{19}(50)+ τC_3-N_2-C_1-C_8(17)
66.			40	39	58	57	τS_{22}-C_{19}-C_{16}-N_2(75)
67.			34	33	34	32	βC_{19}-C_{16}-N_2(18)+ βS_{22}-C_{19}-C_{16}(14)+βCl_{25}-S_{22}-C_{19}(10)+ γC_{19}-C_1-C_3-N_2(44)
68.			27	26	34	33	τC_{19}-C_{16}-N_2-C_1(10)+ τCl_{25}-S_{22}-C_{19}-C_{16}(72)
69.			9	9	5	5	τC_{19}-C_{16}-N_2-C_1(69)+ τCl_{25}-S_{22}-C_{19}-C_{16}(21)

(Stretching – ν, Bending - β, torsion - τ, out of plane bending - γ, very strong-vs, strong-s, medium-m, Weak-w, very weak-vw)

9.5 C–S Vibrations

In the (2-PESC) molecule, the C-S stretching modes are found at wavenumbers 469 and 123 cm^{-1} in the FT-Raman spectrum. The βS-C-C vibrations occur at wavenumbers 621 cm-1 and 123 cm-1 in the FT-Raman region.

9.6 S–Cl Vibrations

The S-Cl group is also highly electrophilic in (2-PESC) molecule. The stretching beats are observed at wavenumbers 378 and 228 cm^{-1} in the FT-Raman region.

9.7 S=O Vibrations

The S=O are present in the sulfonyl chloride group in the molecule 2-phthalimidoethanesulfonyl chloride. The stability of this structure depends on the S=O bonds. In order to create sulfonyl derivatives, the sulfur atom is transformed into a reactive electrophile by the electron-withdrawing activator S=O. The S=O stretching modes are observable at wavenumbers 868 cm^{-1} and 876 cm^{-1} in the FT-IR and FT-Raman region respectively. The βO-S-O oscillations are observed at scaled wavenumber 360 cm^{-1} and 405 cm^{-1} at the 6-311++G(d,p) and cc-pVDZ core level, respectively.

According to the **Table 8**, C=O peaks are obtained at wavenumber 1702 cm^{-1} in the FT-IR spectrum & at 1772 cm^{-1} in the FT-Raman spectrum. The S=O peaks are obtained at 868 cm^{-1} and 876 cm^{-1} in the FT-IR and FT-Raman region respectively. The C-H oscillations are found at 2982 & 2924 cm^{-1} in the FT-IR spectrum and at 2826 cm^{-1} in the FT-Raman spectrum.

The FT-IR spectrum of the molecule is shown in **Figure 4**. Usually, carbonyl (C=O) stretching vibrations occur between 1600 and 1800 cm^{-1}. According to **Figure 4**, one noticeable peak in the experimental spectra, located at 1701.55772 cm^{-1}, is a good indicator of a C=O stretching vibration. In the computational spectra, in the cc-pVDZ basis set, a strong peak is also seen at 1799 cm^{-1}, while in the 6-311++G(d,p) basis set, a very strong peak is visible at 1684 cm^{-1}. The usual range for sulfoxide stretching vibrations is 1000–1070 cm^{-1}. According to **Figure 4**, one peak in the experimental spectrum, located at 1085.60501 cm^{-1}, is marginally beyond the usual range but might represent an S=O signal based on the surroundings and molecular structure. An additional peak in the 1100 cm^{-1} is also observed. There are peaks in the computed spectra at approximately 1113 cm^{-1} and 1164 cm^{-1}. Sulfonyl chloride (SO_2Cl) group shows prominent, distinctive bands between 1410-1370 cm^{-1} and 1204-1166 cm^{-1}.

The Raman spectrum of the molecule is shown in **Figure 5**. As stated before**,** the typical range of the C=O stretching vibration is 1600 to 1850 cm^{-1}. According to **Figure 5**, one peak at 1775 cm^{-1} is found in the experimental spectrum. For S=O (sulfoxide or sulfone) double bond, the usual stretching vibrations fall between 1000 and 1200 cm^{-1}. The experimental spectrum shows a prominent peak at wavenumbers 1011 and 1194 cm^{-1}.

For the sulfonyl chloride group, a peak is observed at 1409 cm^{-1} in the experimental spectrum and at 1364 cm^{-1} computed at 6-311++G(d,p) basis set. These peaks are outside the range and do not exactly match the literature. One aliphatic C-H band appears at 2827 cm^{-1} in the experimental result, and one aromatic C-H band appear at 3080 cm^{-1} in the computed result at 6-311++G(d,p) basis set. Here, only the prominent peaks are discussed, and all other peaks are given in **Table 8**.

10. Conclusion

In this paper, 2-phthalimidoethanesulfonyl chloride, a physiologically active chemical compound, is computationally studied. Density functional theory (DFT) is used to explore the molecule theoretically at the B3LYP level using the 6-311++G(d,p) and cc-pVDZ sets. The optimal bond lengths and angles are determined using the DFT computations. Calculations are performed for the molecule's specific heat, entropy and enthalpy for temperatures between 100 and 1000 Kelvin. Using an appropriate scaling factor, the calculated and observed vibrational frequency values agree with one another. FT-IR and FT-Raman spectra are recorded in a suitable range. By using Natural Bond Orbital (NBO) analysis, the molecule (2-

PESC)'s intramolecular and intermolecular interactions are confirmed. The molecule does not have good NLO properties, as indicated by its lower value of first-order hyperpolarizability. 2-Phthalimidoethanesulfonyl chloride is a unique chemical intermediate that is mostly utilized as a reagent and in the pharmaceutical industry to create sophisticated medicinal compounds. So, the present study of the studied molecule can act as a database to analyse this molecule for various applications. Lastly, the mulliken charge distribution has also been done. This study explores the impact of structural modifications on the spectroscopic properties of the molecule, contributing to the development of more effective pharmaceutical agents. These results will be useful for researching this molecule in various ways.

Conflicts of Interest

No conflict of interest was reported by the authors regarding the publication of this paper.

Acknowledgments

There was no specific grant awarded for this study by public, private, or nonprofit funding organizations. The authors would like to thank the Physics Department, Chaudhary Charan Singh University, Meerut for the Raman characterization.

AI Disclosure

The author(s) declare that no assistance is taken from generative AI to write this article.

References

Akgün, H., Karamelekoğlu, İ., Berk, B., Kurnaz, I., Sarıbıyık, G., Öktem, S., & Kocagöz, T. (2012). Synthesis and antimycobacterial activity of some phthalimide derivatives. *Bioorganic & Medicinal Chemistry*, *20*(13), 4149-4154. https://doi.org/10.1016/j.bmc.2012.04.060.

Annu, Yadav, B.S., Teotia, J., Uppadhayay, R.K., Rathi, I., & Kumar, V. (2022). Vibrational spectral studies, thermodynamic investigations and DFT (NLO, NBO, MEP) computation of benzene derivative. In *Proceedings of the International Conference on Atomic, Molecular, Optical & Nano Physics with Applications: CAMNP 2019* (pp. 463-485). Springer, Singapore. https://doi.org/10.1007/978-981-16-7691-8_44.

Aswathy, P., Joe, I.H., Narayana, B., Sarojini, B.K., Harshitha, K.R., & Monicka, J.C. (2025). Spectroscopic and theoretical investigations of solvent-dependent NLO properties of thiophene-thiazole based push-pull chromophores. *Journal of Molecular Structure*, *1345*, 143026. https://doi.org/10.1016/j.molstruc.2025.143026.

Aygün, M., Celepci, D.B., Akgül, Ö., & Pabuccuoglu, V. (2024). Single-crystal X-ray structure, theoretical (Hirshfeld, electronic properties, NBO, NLO, RDG), and molecular docking studies of three phthalimidoethanesulfonamide derivatives. *Journal of Molecular Structure*, *1317*, 139094. https://doi.org/10.1016/j.molstruc.2024.139094.

Balachandran, V., Lalitha, S., & Rajeswari, S. (2012). Density functional theory, comparative vibrational spectroscopic studies, NBO, HOMO–LUMO analyses and thermodynamic functions of N-(bromomethyl) phthalimide and N-(chloromethyl) phthalimide. *Spectrochimica Acta Part A: Molecular and Biomolecular Spectroscopy*, *91*, 146-157. https://doi.org/10.1016/j.saa.2012.01.034.

Colthup, B.N., Daly, H.L., & Wiberley, E.S. (2012). Introduction to infrared and Raman spectroscopy (Third Edition). Elsevier. New York, USA.

Daina, A., Michielin, O., & Zoete, V. (2017). SwissADME: a free web tool to evaluate pharmacokinetics, drug-likeness and medicinal chemistry friendliness of small molecules. *Scientific Reports*, *7*(1), 42717. https://doi.org/10.1038/srep42717.

Doraghi, F., Morshedsolouk, M.H., Zahedi, N.A., Larijani, B., & Mahdavi, M. (2024). Phthalimides: developments in synthesis and functionalization. *RSC Advances*, *14*(32), 22809-22827. https://doi.org/10.1039/d4ra03859b.

Evecen, M., Duru, G., Tanak, H., & Ağar, A.A. (2016). Synthesis, crystal structure, spectral analysis and DFT computational studies on a novel isoindoline derivative. *Journal of Molecular Structure*, *1118*, 1-9. https://doi.org/10.1016/j.molstruc.2016.03.079.

Foster, J.P., & Weinhold, F. (1980). Natural hybrid orbitals. *Journal of the American Chemical Society*, *102*(24), 7211-7218. https://doi.org/10.1021/ja00544a007.

Jamróz, M.H. (2013). Vibrational energy distribution analysis (VEDA): scopes and limitations. *Spectrochimica Acta Part A: Molecular and Biomolecular Spectroscopy*, *114*, 220-230. https://doi.org/10.1016/j.saa.2013.05.096.

Karthick, T., Balachandran, V., Perumal, S., & Nataraj, A. (2011). Rotational isomers, vibrational assignments, HOMO–LUMO, NLO properties and molecular electrostatic potential surface of N-(2 bromoethyl) phthalimide. *Journal of Molecular Structure*, *1005*(1-3), 202-213. https://doi.org/10.1016/j.molstruc.2011.08.051.

Krishnakumar, V., Balachandran, V., & Chithambarathanu, T. (2005). Density functional theory study of the FT-IR spectra of phthalimide and N-bromophthalimide. *Spectrochimica Acta Part A: Molecular and Biomolecular Spectroscopy*, *62*(4-5), 918-925. https://doi.org/10.1016/j.saa.2005.02.051.

Kumar, S., Surbhi, & Yadav, M.K. (2018). Vibrational spectroscopic investigation, first hyper polarizability and homo–lumo analysis of tetrahydroxy-1, 4quinone hydrate using density functional theory and hartree-fock method. *Russian Journal of Physical Chemistry B*, *12*(3), 383-393. https://doi.org/10.1134/S1990793118030132.

Kumar, V., Teotia, J., & Yadav, A.K. (2022). Vibrational (FT-Raman and FTIR) spectroscopic study, molecular structure, thermodynamic properties and non-linear optical properties of benzyl-3-oxopyperazine-1-carboxylate by density functional theory. *Materials Today: Proceedings*, *62*, 7137-7141. https://doi.org/10.1016/j.matpr.2022.02.185.

Kushwaha, N., & Kaushik, D. (2016). Recent advances and future prospects of phthalimide derivatives. *Journal of Applied Pharmaceutical Science*, *6*(3), 159-171. https://doi.org/10.7324/JAPS.2016.60330.

Lee, C., Yang, W., & Parr, R.G. (1988). Development of the Colle-Salvetti correlation-energy formula into a functional of the electron density. *Physical Review B*, *37*(2), 785-789. https://doi.org/10.1103/PhysRevB.37.785.

Leela, J.S.P.P., Hemamalini, R., Muthu, S., & Al-Saadi, A.A. (2015). Spectroscopic investigation (FTIR spectrum), NBO, HOMO–LUMO energies, NLO and thermodynamic properties of 8-Methyl-N-vanillyl-6-nonenamideby DFT methods. *Spectrochimica Acta Part A: Molecular and Biomolecular Spectroscopy*, *146*, 177-186. https://doi.org/10.1016/j.saa.2015.03.027.

Lipinski, C.A. (2004). Lead-and drug-like compounds: the rule-of-five revolution. *Drug Discovery Today: Technologies*, *1*(4), 337-341. https://doi.org/10.1016/j.ddtec.2004.11.007.

Reed, A.E., & Weinhold, F. (1983). Natural bond orbital analysis of near-Hartree–Fock water dimer. *The Journal of Chemical Physics*, *78*(6), 4066-4073. https://doi.org/10.1063/1.445134.

Reed, A.E., & Weinhold, F. (1985). Natural localized molecular orbitals. *The Journal of Chemical Physics*, *83*(4), 1736-1740.

Reed, A.E., Weinstock, R.B., & Weinhold, F. (1985). Natural population analysis. *The Journal of Chemical Physics*, *83*(2), 735-746. https://doi.org/10.1063/1.449486.

Reeda, V.J., & Jothy, V.B. (2023). Vibrational spectroscopic, quantum computational (DFT), reactivity (ELF, LOL and Fukui), molecular docking studies and molecular dynamic simulation on (6-methoxy-2-oxo-2H-chromen-4-yl) methyl morpholine-4-carbodithioate. *Journal of Molecular Liquids*, *371*, 121147. https://doi.org/10.1016/j.molliq.2022.121147.

Santos, J.L., Yamasaki, P.R., Chin, C.M., Takashi, C.H., Pavan, F.R., & Leite, C.Q. (2009). Synthesis and in vitro anti Mycobacterium tuberculosis activity of a series of phthalimide derivatives. *Bioorganic & Medicinal Chemistry*, *17*(11), 3795-3799. https://doi.org/10.1016/j.bmc.2009.04.042.

Sharma, U., Kumar, P., Kumar, N., & Singh, B. (2010). Recent advances in the chemistry of phthalimide analogues and their therapeutic potential. *Mini Reviews in Medicinal Chemistry*, *10*(8), 678-704. https://doi.org/10.2174/138955710791572442.

Teotia, J., Annu, Rathi, I., Bhardwaj, S., Uppadhayay, R.K., & Garg, A. (2022). Vibrational (FT-IR and FT-Raman) spectroscopic investigations, NLO, NBO and MEP analysis of 1, 4-dibromo-2, 5-dimethoxybenzene by DFT. In *Proceedings of the International Conference on Atomic, Molecular, Optical & Nano Physics with Applications: CAMNP 2019* (pp. 439-462). Springer, Singapore. https://doi.org/10.1007/978-981-16-7691-8_43.

Teotia, J., Kumar, S., Kumar, R., & Yadav, M.K. (2016). Ultraviolet absorption spectra, solvent effect and non-linear optical properties of 2-Amino-4, 6-dimethylpyridine by hartee-fock and density functional theory. *Asian Journal of Chemistry*, *28*(10), 2204. https://doi.org/10.14233/ajchem.2016.19928.

Udayappan, V., Easwaramoorthy, D., Aravindhan, S., & Asok, A.A. (2024). Experimental and theoretical vibrational analysis, structural conformations, DFT estimations, antibacterial, antifungal, DPPH, H2O2, Nitric oxide scavenging activity drug, in silico molecular docking, and ADMET studies of N-(2-carboxylphenyl) phthalimide (CPPD). *Journal of Molecular Liquids*, *414*, 126119. https://doi.org/10.1016/j.molliq.2024.126119.

Weinhold, F. (2001). A new twist on molecular shape. *Nature*, *411*(6837), 539-541. https://doi.org/10.1038/35079225.

Weinhold, F., & Landis, C.R. (2005). *Valency and bonding: a natural bond orbital donor-acceptor perspective*. Cambridge University Press. Cambridge , UK.

Yadav, B., Singh, A., Teotia, J., Kumar, V., Saran, R., & Teotia, D. (2023). Structural parameters, NLO properties, thermodynamic functions, NBO analysis and fukui functions of benzyl (3-Fluoro-4-Morpholinophenyl) carbamate by density functional theory. *Journal of Pharmaceutical Negative Results*, *407*, 1285-1293. https://doi.org/10.47750/pnr.2023.14.S01.175.

Yadav, B.S., Garg, A., Teotia, J., & Bhardwaj, S. (2022). Electronic solvation (UV-Vis) and NLO properties of 2-chloroanthraquinone: an experimental and computational modeling approach. In *Proceedings of the International Conference on Atomic, Molecular, Optical & Nano Physics with Applications: CAMNP 2019* (pp. 563-574). Springer, Singapore. https://doi.org/10.1007/978-981-16-7691-8_54.